A Fast and Simple Method for Designing a Linear Induction Motor (LIM)

BEKADDOUR BENATIA Mostefa[1,2], BEKKOUCHE Benaissa [2], MERAHI Amir [1] , MEDLES Karim [1]
[1]Electrostatics and High Voltage Research Unit IRECOM, University Djillali Liabès of Sidi Bel Abbès 22000, Algeria
[2]Signals and Systems Laboratory Research University , Abdelhamid IbnBadis of Mostaganem, , Algeria

Mail: kmedles@gmail.com

Abstract - *This paper presents a simple and fast methodology for designing a linear induction motor (LIM). The method consists in expressing the mechanical output parameters of the machine such as the thrust force and power as a function of the progression of the geometric dimensions of a known LIM model chosen as reference. The approach consists in several steps, starting with the choice of prototype, and the analysis of its mechanical characteristics. COMSOL MultiPhysics is an indispensable tool in this research to simulate a multitude of variants, to ensure the magnetization of the machine. Then the operation of a variant of a linear motor was designed. The results obtained are very satisfactory.*

Key words: *COMSOL, Linear Motor, Thrust force.*

1. Introduction

The design of electrical machinery using the finite element method (FEM) provides calculation results clos to reality. The difficulty of studying electrical machines by FEM lies in the juxtaposition of several magnetic phenomena [1-4]. This article is in a perspective to facilitate the motor design by a simple and fast approach. Linear induction motors (LIM) are more robust and have high reliability than rotating motors due to the small number of components. [4-9]. In general the design of an electrical machine consists in several steps. It begins with the choice of the prototype, and the domain of variation of its geometry, it continues with the analysis of the electrical magnetic and mechanical characteristics of each variant. Finally a case study was carried out. Numerical methods of calculation allowed several simulations and quick comparisons between various variants, using COMSOL Multi-physics, based on the finite element method [10-15]. The simplicity of the digital tool offers a good time saving for researchers to produce results that can be easily exploited by the manufacturers.

2- The algorithm of the design methodology

The development of digital computing tools in recent decades allows a great simplification of the design and engineering of electrical machines. In this context, a methodology is introduced to facilitate the work of engineers in charge with the design of linear induction motors. This method, which based on the algorithm presented hereafter, can be generalized to other types of electrical machines.

ALGORITHM

1. Choose a real prototype with known design features as a reference;
2. Validate the operating characteristics of the reference prototype using an appropriate design software like COMSOL MultiPhysics;
3. Vary the geometric parameters of the prototype and predict the performances of the modifies motors;
4. Perform the magneto-static and magneto-dynamic study of the new models;
5. Confirm the operational features of new models ;
7. Draw the graphs of the thrust force and the power of the new models, as functions of the rates of geometric variation.
8. Perform a detailed case study of the chosen model.

The execution of this algorithm takes time, however, the computing capability of Multi-Physics COMSOL software simplifies the task.

3. Overview of the simulation software

The numerical simulation software used in this work is COMSOL Multi-Physics, which is based on the finite element method. It allows to model and to simulate different physical phenomena for complex geometries thanks to the richness of its database and the speed of calculation. [5-8].

A. Electromagnetic Equations

The device is characterized by a 3D electromagnetic equation in terms of the steady-state magnetic vector potential $\overrightarrow{A}$:

$$\nabla^2 \vec{A} = -\mu \vec{J}_s + \sigma\mu \left(\frac{\partial \vec{A}}{\partial t} - \vec{v} \times \overrightarrow{rot}(\vec{A})\right) - \overrightarrow{rot}(\vec{M}) \qquad (1)$$

where; σ: Conductivity, μ: Permeability of the material, $\vec{J}_s$: Density of the current in the coil, $\vec{v}$: Mechanical velocity, $\vec{M}$: Magnetization

B. Expression of Electromagnetic Force

The force F_z is calculated in COMSOL by integrating the z component of Maxwell's magnetic tensor on the central magnet surface [11-14]:

$$F_z = \iint_s \left[(n.H).B^T - \frac{1}{2}n.(H.B)dA\right] \quad (2)$$

The electric power of the motor is defined by

$$P_z = F_z.v \quad (3)$$

where n is the outward normal from the magnet.

C. Boundary Conditions

The software COMSOL Multi-physics require boundary conditions of Dirichlet (A=0, V=0) or Neumann $(\frac{\delta A}{\delta n} = 0)$ type on the overall geometry of the domain selected as application. In the present case, the boundary conditions of the computational model are defined in such a way that the contour of the model is magnetically isolated. Continuity is ensured between all the active elements of the machine in order to allow the closing of the magnetic field lines. Moreover, the magnetic symmetry of electrical machines allows to makethe calculations in only half of the domain.

4 – Simulation :

1. The choice of reference motor

The prototype chosen is a linear motor LMG05-030 [1]. It was studied by the Electrical and Electronics Power Laboratory (L2EP), in cooperation with the China Scholarship Council (CSC). The analysis and simulation of this motor was made by Vector Fields Software [1]. The secondary of the machine is made by an infinite aluminum plate placed between the two primaries [1]. The device is intended for a railway application, where the aluminum plate is fixed to the ground, to form a third rail, while the primary part is movable, installed on the train (Fig 1-a).

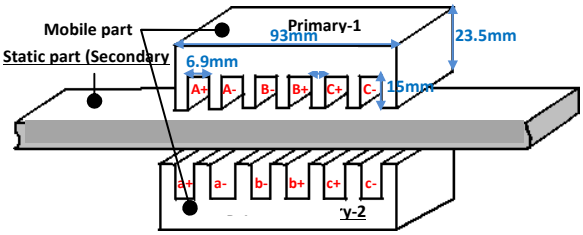

Fig 1-a.A linear motor LMG05-030 [1]

The primary contains six notches with 210 conductors per notch. The three windings are wound in a concentrated manner as shown in Fig (1-b). The performance of the LMG05-30 motor is presented in Appendix A

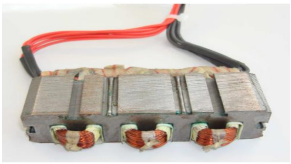

Fig1-b : Construction of a primary

1. Presentation of the motor reference in COMSOL

The geometry presented by COMSOL is shown in Fig. 2a

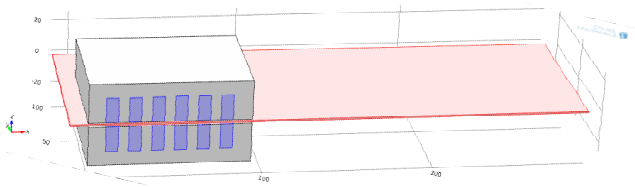

Fig 2-a the geometry in COMSOL

The entire mesh of the machine consists of 246429 elements (Fig. 2b)

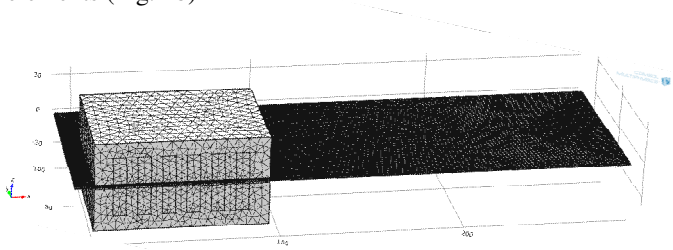

Fig 2-b the Mesh in COMSOL

2. Validation by COMSOL:

To validate the characteristics of the reference motor that will serve as a basis for our design,the characteristics of the model simulated by the COMSOL software were compared to that determined by Vector Fields software **[1]**, as shown in Fig. 3, 4 and5.

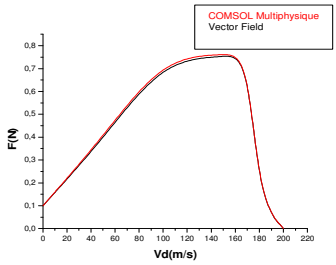

Fig.3. the pushing force as a function of the traveling speed

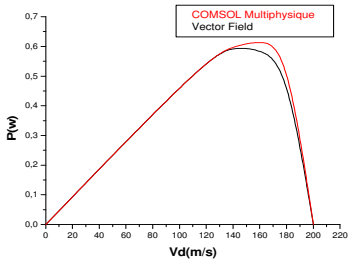

Fig 4.the electric power as a function of travel speed

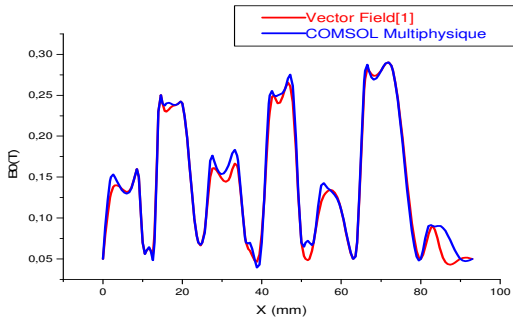

Fig.5. Magnetic induction in the air gap

5. Interpretation:

The analysis of the values and the waveform of Figs 3, 4 and 5 shows that the curves of the displacement force, the electric Power and the induction calculated by the multi-physical COMSOL software are the same as determined by the Vector Fields [COBHAM] software shown in [1]. The results show a great coherence which presents us a clement manometer to adopt the parameters of this motor as the basis of our approach to design and reassure us on our good use of multi physics software that presents the mill of this approach.

1. Variation of geometric parameters

After certifying the characteristics of the prototype and validated calculation program, we started the operation of varying the geometry of the machine, step by step. For the first step we have enlarged the dimensions of the motor reference in two times with a prediction the necessary current. For the prediction of the current as indicated in the third step of the algorithm, we kept the same number of notches and the same number of turns N per slot as the same construction material of the prototype. However the current will be determined approximately from the variation of the cross-section of the notches which is generally defined in construction, as follows:

$$S = N.C_0.A \qquad (4)$$

With: C_0: The coefficient of filling, A: Conductor cross section

- The prototype motor

$$S_1 = N.C_0.A_1 \qquad (5)$$

- The section of the new model notch is defined by;

$$S_2 = N.C_0.A_2 \qquad (6)$$

- The cross-section of the conductor A2 is given by;

$$A_2 = \frac{S_2}{N.C_0} \qquad (7)$$

The change in cross section of the conductor imposes a variation of current of the coil. This is defined by;

$$I_2 = \frac{A_2 * l_1}{A_1 * l_2} . I_1 \qquad (8)$$

This prediction allows us to determine the operating characteristics of the new MILs and the study of its magnetic regime [17].

2. Magnetic analysis

The study of the magnetic behavior of the material chosen for the realization of the prototype takes an important place in our design process as indicated in step 5 of our algorithm. The confirmation of the variant characteristics results is automatically followed by a magneto static and magneto dynamic examination of the material in order to have information on the variation of the magnetic flux density and the permeability. The COMSOL software by these powerful options, it allows us to have these expertise. For each variant, the analysis is performed for the two magnetic behaviors cited above and for two distinct and sensitive geometrical spaces of the magnetic circuit. The first geometric space represents the middle axis of the stator breech, which represents the mean line of the flux. The second geometric space represents the axis that passes through 1/3 of the primary teeth. Figs 6, 7, 8 and 9 show this variation for the reference model and for the fifth geometry model.

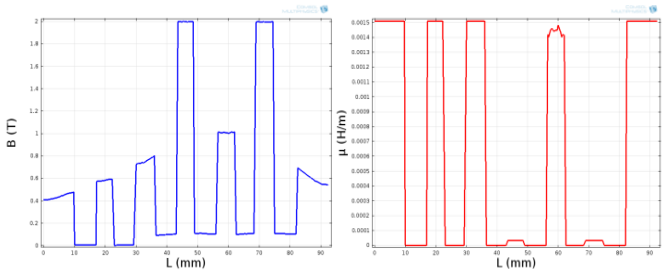

Fig 6-a: B=f (L)and μ=f (L) at 1/3 of the teeth of the primary, MIL Reference for t = 0s

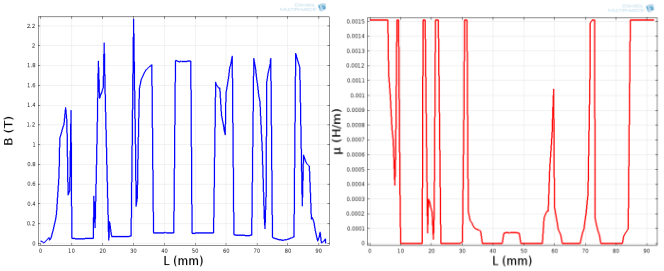

Fig 6-b: B =f (L) and μ=f (L) at 1/3 of the teeth of the primary, MIL Reference for t = 1s

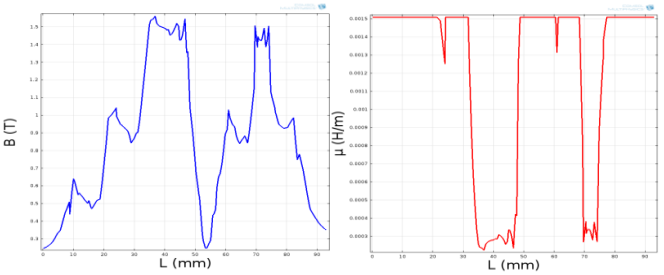

Fig 7-a: B =f (L) and μ=f (L) at the primary yoke of MIL Reference for t = 0s

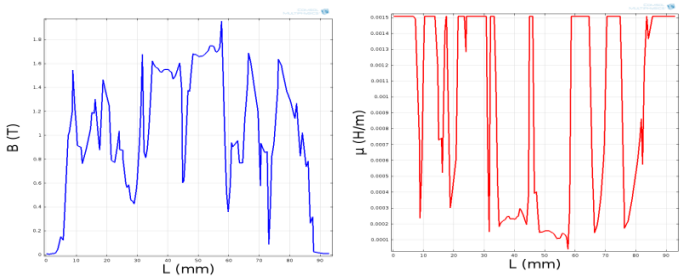

Fig 7-b: B =f (L) and μ=f (L) at the primary yoke of MIL Reference for t = 1s

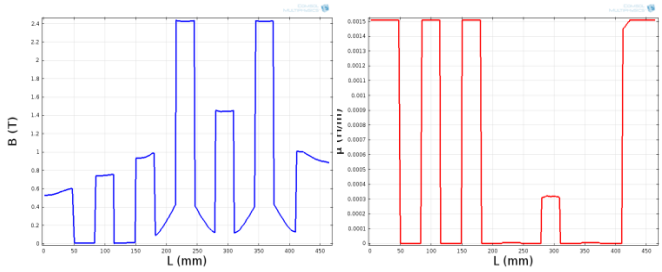

Fig 8-a: B=f (L) and μ=f (L) at the level of 1/3 of the teeth of the primary of the geometry **5** for t = 0s

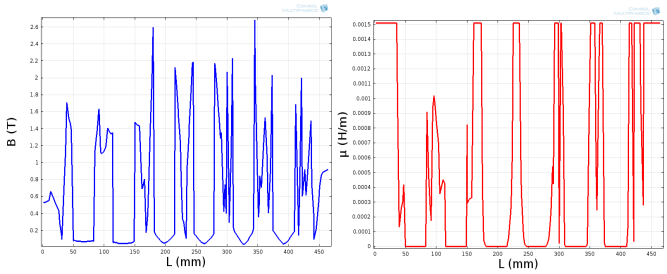

Fig 8- b: B=f (L) and μ=f (L) at the level of 1/3 of the teeth of the primary of the geometry **5** for t = 1s

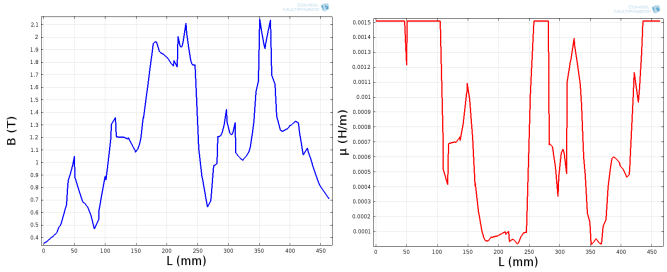

Fig 9-a: B =f (L) and μ=f (L) at the primary yoke of the geometry **5** for t = 0 s

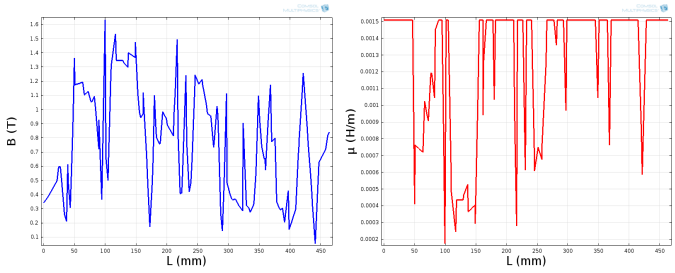

Fig 9-b: B=f (L) and μ =f (L) at the primary yoke of the geometry **5** for t = 1s

After carrying out the magnetostatic and magnetodynamic examination of the geometry, an analysis of the characteristics and a confirmation of operation will be approved out by the software.

3. 3- Validation of the operation of the geometric variant

The operating characteristics of the new LIMs will be compared in waveform and the pace and amplitude values. However, if the judgment is acceptable one passes to the sixth loop of algorithm where the dimensions increase to three times and joins the third loop of the algorithm, in order to realize the second step. The use and enrichment of the COMSOL software allows us to make several simulations with progressive geometries. We have performed the simulation of seven geometries, as shown in Figs 10, 11 and 12.

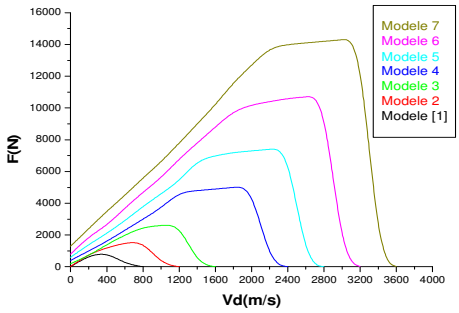

Fig 10 Evolution of force depending on travel speed

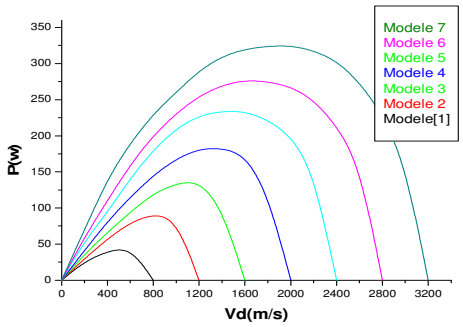

Fig.11 Change in power as a function of travel speed

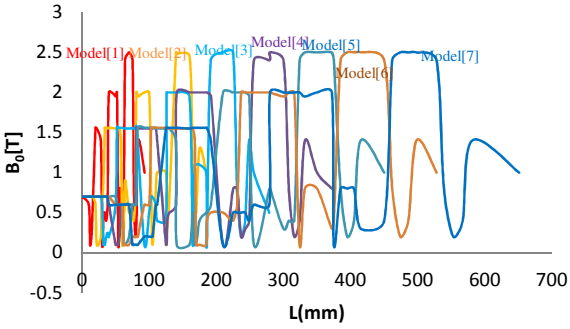

Fig.12 Representation of B = f (L) at the air gap

The operating characteristics of all the geometries presented by COMSOL well show a concordance of the output parameters of the new geometries with that of the reference motor is like watches in Figs 10,11 and 12. This diagnosis presents an index, of good functioning of the new geometries.

The two Figs (6-a, b) and (7-a, b) show the variation of the density of the magnetic flux and of the permeability as a function of the geometry for the construction material of the reference motor. Figs (8-a, b) and (9-a, b) show those of the Fifth model for the same construction material. As a remark for the magneto static and magneto dynamic states, the variation is almost identical for all the geometries. This shows that the distribution of the magnetic field and the level of saturation despite their small variations remains acceptable and favor the conduct of the magnetic flux lines. This symbolizes an indication of good magnetization of each new machine.

It can also be seen in Figs 10, 11 and 12 that the waveforms of the displacement force curves and the electric power of the new geometries as a function of the displacement speed retain identical shapes as that of the reference prototype. Concerning the amplitude of these magnitudes and the speed vary clearly proportional to the geometry. This correlation presents good information, of excellent functioning of the new geometries of the LIMs conceived. The graphs of the magnetic induction in the air gap of Figure12 show that the variation of the induction is the same for the motors. It has a good index of the saturation regime and also gives us information on the distribution of the field Magnetic and magnetizations of cloned machines.
Therefore, according to the different results presented, we find that the new linear motors designed work, ensuring greater mechanical quantities of outputs with a minimum increase in volume of the machine.

4. Construction characteristics

The study of the results of each model clearly showed the proportionality between the mechanical quantities and the geometric variation of the motor.

So the seventh loop of the algorithm of the method is devoted to a small application which regroups all the caution points of the different simulations. This manipulation allows us to plot graphs of the variation of the pushing force and the electric power depending on the multiplier of geometric dimension as shown in Fig 13. This approximate approach makes it easier for the constructor to define the volume of his new machine from the mechanical output variables defined by the customer variables defined by the customer. It can be generalization for another type of machine even for the inverse case of a large prototype one can deduce a minimization of the model.

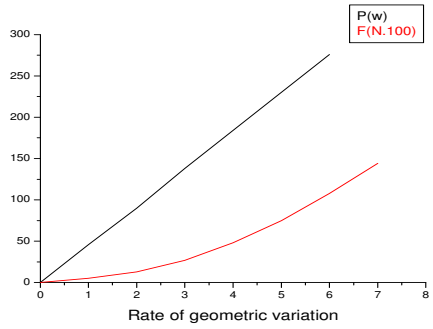

Fig.13. Variation of F(N) and P(W) as a function of geometric rate of change

We hope that the results of this methodology are acceptable and facilitate the work of the manufacturers and develop the industry of these linear machines.

5. Confirmation of operation of a model for the realization

1- Analysis of mechanical characteristics

To verify the skills of our approach and make a realization we have a confirmation process of how a MIL designed following the approach defined by the graphs of Figs 13.
We chose from the curve a push force greater than five times the strength of the reference prototype, which represents on the curve an increase in geometry twice the reference motor.

When applying the new motor data to the COMSOL we obtained the following results:

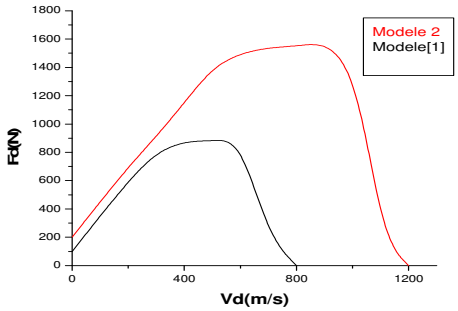

Fig.14 Comparison of the new model F = f (V_d) with [1]

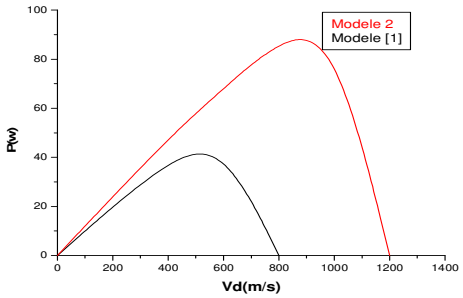

Fig.15 Comparison of the new model P = f (V_d) with [1]

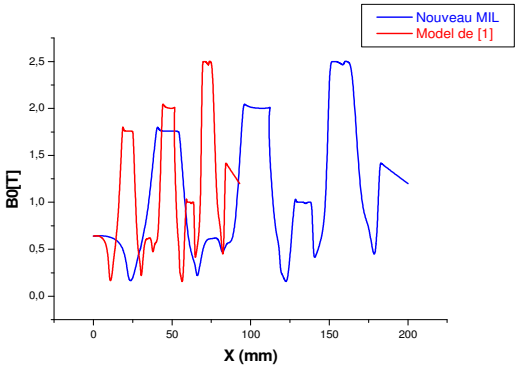

Fig.16 Comparison of the new model B = f (X) with [1]

It is noted in Figs 14, 15 and 16 paces and that the shapes of the curves keep identical shapes as the reference prototype, which has an index of proper functioning of MIL designed. Regarding the magnitude of the force is 5.33 times greater than the force of the MIL reference. However, the speed has greatly increased that justify the operation of our model designed.
The graphs of the magnetic induction in the air gap shown in the Fig 17 shows that the variation of induction is the same for both motors .It has a good indicator of the saturation regime of our designed model and also gives us information's on the distribution of the magnetic field. This distribution is proportional to the variation of the motor geometry within the limits of our proposed approach.

2- The Confirmation of Operation of the Model Designed in 3D

To validate the operation of the model after the design, the COMSOL offers us the possibility to analyze several parameters of the machine.

However, we have chosen three essential characteristics, and indicators of the functioning. For this work we limited the simulation on this variant to deepen our analysis of functioning because one cannot make a decision if not by the internal anatomy of the machine.

-The first represents the distribution of the flux density in the magnetic circuit which presents a gauge of the machine magnetization and the transfer of energy between the different parts of the machine.

-The second is summed up in the analysis of the mechanical characteristic which symbolizes the baroscopic of movement and the translation of armatures.

- The third study concerns the variation of the magnetic field in the air gap and the distribution of the eddy currents in the fixed armature which present the index of interaction inside the models designed.

3- Field conFig ration Given by COMSOL

The magneto-graphic study of the distribution of field in the magnetic circuit of a designed machine provides several basics information about all active parties. The flux behavior, saturation and it shows the geometric points weak [18-21]. Therefore, the field distribution reflected an image of motor operation.

The 17, 18 and 19 Figs show the density distribution of magnetic flux of the new motor. The analysis shows that the teeth of the stator are saturated in the vicinity of 2 Tesla and does not exceed 2.5 Tesla in the most saturated places. Concerning the maximum inductions, they are located mainly in the polar expansions.

From this comparison of these Figs it can be see that the magnetic field lines pass through the air gap and the rotor. This explains the phenomenon of energy transfer between the moving coil inductor and the fixed plate. This explains the phenomenon of energy transfer between the moving coil inductor and the fixed plate. This explains the existence of an interaction between the stator field and the rotor field. The displacement of the level of saturation from one tooth to the other as a function of time confirms that the distribution is dynamic and even periodic this gives us a generous indication of the operation of the machine.

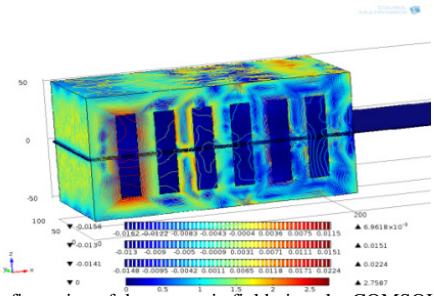

Fig 17: Configuration of the magnetic field given by COMSOL (t = 0s)

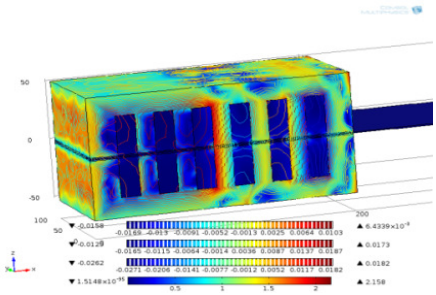

Fig 18: Configuration of the magnetic field given by COMSOL (t=0.009s)

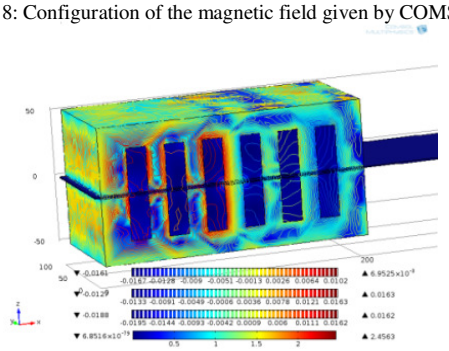

Fig 19 Configuration of the magnetic field given by COMSOL (t=0.02s)

4- Displacement force

Fig 20 shows the mechanical characteristic of the machine for voltage and frequency supply (380V / 50Hz).

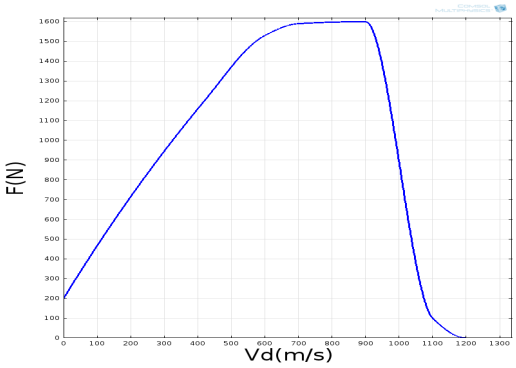

Fig 20: F = f (V_d) of the machine designed

In remarks that the pushing force applied to the secondary first increases with speed. Then when the speed is in the vicinity of 900m/s, the thrust force reaches its maximum value and then decreases until cancellation .This model has a mechanical characteristic similar to that of the rotary induction motor. We can deduce that the maximum of the force varies as a function of the nominal frequency, which confirms the functioning of the model

5- The flux inside the air gap

Fig 21 shows the amplitude of the induction in the air gap.

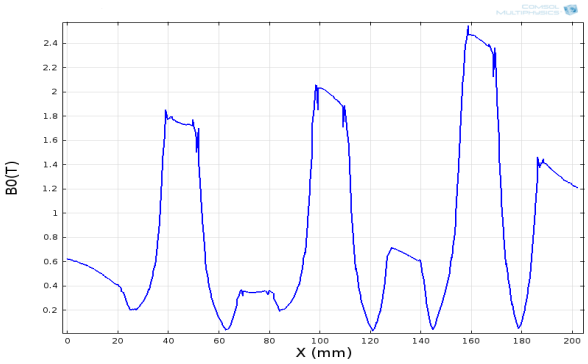

Fig 21: The variation of the magnetic induction in the air gap

The distribution of the amplitude of the induction in the air gap makes it possible to demonstrate the effect fo longitudinal ends, the induction in the air gap is not uniform. It is stronger at the output of the motor than at the input. The curve peaks correspond to the positions of the teeth of the primary. The difference between these values makes it possible to show up the effects of the slot openings and the winding. The variation of this curve reflects the non-uniformity of the air gap

6- Distribution of eddy currents in the rotor

Fig 22 shows the distribution of eddy currents for a position in direction X.

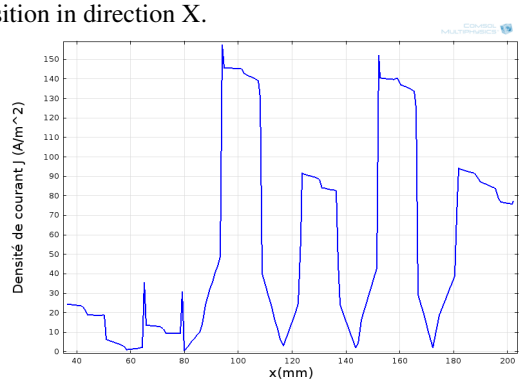

Fig 22: Current density in the rotor (t = 0, f = 50Hz)

This curve shows firstly the existence of the magnetization in the machine and especially the secondary. On the other hand, the non-uniformity of the current along the X direction reflects the distribution of the magnetic field and justifies that the effect of these electric currents is limited at the level of the core.

The analysis of the Fig 20, 21 and 22 obtained by the COMSOL software used in our design gives real symptoms of operation of the models.

So according to the different results presented, we find that the new LIM designed on the basis of the abacus of Figs 13 works on ensuring a greater thrust force with a minimum increase of volume of the machine.

From the literature, several scientific studies has been published on the development of methods of design of electrical machines, the majority of these approaches treat the machine operation and performances, taking into account a fixed geometry.

6. CONCLUSION

This paper presents a very simple methodology to facilitate the design of a linear induction motor. The methodology is based on the choice of an existing prototype, to serve as reference. The geometry of the model is then varied and the operating characteristics of the modified motors are analyzed, using COMSOL Multi-Physics software.. This cloning operation allows the plot a function linking the mechanical parameters of the motor with its geometric dimensions.

Finally, the work was completed by a simulation of the operation of a motor model chosen according to the determined approach (Fig 13). The results obtained represent good indicators of the functioning of this variant. After the confirmation of the model our laboratory decided to make the realization of this new motor for the continuity of the research.

I

REFERENCES

1. Gong, J., Gillon, F., Brochet, P., *Magnetic and Thermal 3D Finite Element Model of a Linear Induction Motor*. In: Conference Vehicle Power and Propulsion, Lille, French, September 2010.
2. Baluta, G.: *FEM Analysis of Brushless DC Servomotor with Fractional Number of Slots per Pole,* In: IEEE Trans. Electron Devices, (2014), Vol.14, Fev 2014, p. 103-108.
3. Ungureanu, C.: *FEM Analysis of a New Electromechanical Converter with Rolling Rotor and Axial Air-Gap,* In: IEEE Trans. Electron Devices, (2014), Vol. 15, Nov2014, pp. 69-74.
4. Baluta, G.: *FEM Analysis of Brushless DC Servomotor with Fractional Number of Slots per Pole,* In: IEEE Trans. Electron Devices (2016), Vol. 16, Aug 2016, pp.25-30.
5. Hellinger, R., Mnich, P.: *Linear Motor-Powered Transportation: History*, Proceedings of the Status, and Future Outlook, IEEE proceedings , November 2009, Vol. 97, pp. 1982-1900.
6. Ghislain, R, *Modélisation et Identification des Forces Electromotrices Non Sinusoïdales, Application à un Moteur Linéaire Synchrone à Aimants Permanents*. In: Proceedings of JCGE'05, 7 et 8 juin 2005, Montpellier French.
7. Zeng, J., Remy, G., Degobert, P., Barre, P.: *Thrust Control of the Permanent Magnet Linear Synchronous Motor with Multi-Frequency Resonant Controllers*. In: Proceedings of 18th International Conference on Magnetically Levitated Systems and Linear Drives, MAGLEV'2004, October 26-28.
8. Gieras, J.F., Piech, Z.J.: *Linear Synchronous Motors: Transportation and Automation Systems*, Editor CRC Press, Sept. 1999.
9. Gieras, J.F.: *Status of Linear Motors in the United States*. In: Proceedings of he 4th International Symposium on Linear Drives for Industry Applications, LDIA2003, Birmingham, UK, 8-10 Sept 2003
10. Merahi, A., Medles, K., Tilmatine, A.: *Design and development of a low cost technique for sorting household*

wastes using eddy current, In: International Journal of Environmental Studies (2016), Vol.73, No.2, p.203-213.
11. COMSOL Multiphysics, *User's guide, AC/DC Module* – User's guide
12. Chebak, A., Viarouge, P., Cros, J.: *Analytical computation of the full load magnetic losses in the soft magnetic composite stator of high-speed slotless PM machines States*. In: Proceedings of IEEE Conference on Electromagnetic Field Computation, Greece, May 2008.
13. Viorel, I. A.: *On the Carter's Factor Calculation for Slotted Electric Machines*. In: IEEE Trans. Electron Devices (2007), Vol.7 , Nov 2007, p. 55-58.
14. Remy, G., Krebs, A., Tounzi, P.J.: *Finite Element Analysis of a PMLSM (part 1) - Meshing techniques and thrust computations*. *States*. In: Proceedings of LDIA 2007, 6th International Symposium on Linear Drives for Industrial Applications, Lille, France, Sept. 2007.
15. Benatia, B., Fatima,B. : *New Geometrical Approach for the Air-gap Reluctance Calculation for the Design of the Machines by the Flow Lines* Method. In: JEEE (2012) , Vol. 5, No 2, October 2012.
16. Bekkouche, B., Chaouch, A., Mezari, Y.: *A Switched Reluctance Motors Analyse Using Permeance Network Method*. In: International Journal Of Applied Motorering Research (2006), Vol.1, No 2, p.137-152.
17. Denkena. B., Imiela. J,: *Current of the linear motor-based condition monitoring in milling*. In: Proceedings of Robotics, Intelligent Systems and Signal Processing 2003. Vol. 1, pp. 559-564, 8-13 Oct. 2003.
18. Polinder, H., Slootweg, J.G., Compter, J.C., Hoeijmakers, M.J.: *Modeling a linear PM motor including magnetic saturation* Power. In: Proceedings of Electronics, Machines and Drives, 2002, p. 632-637, 4-7 June 2002.
19. Boldea, I., Nasar, S.A.: *Linear Motion Electromagnetic Devices*. In: Taylor & Francis, 1990.
20. Polinder, H., Slootweg, J.G., Hoeijmakers, M.J., Compter, J.C.: *Modeling of a linear PM Machine including magnetic saturation and end effects: maximum force-to-current ratio*. In: Industry Applications, IEEE Transactions (2003), Vol. 39, No. 6, pp. 1681-1688, Nov.-Dec. 2003.
21. O'Handley, R.: *Modern Magnetic Materials: Principles and Applications.* Editeur Wiley, New York, 2000.

Appendix 1

The geometric parameters
Non-variable parameters
Number of phases m = 3
Number of pole pairs P = 1
Number of turns per phase N = 210
Number of notches n_e= 6
Thickness of the air gap e = 0.8 [mm]
Plate thickness hp_s = 1 [mm]

Components	Model [1]	Model (2)	Model (3)	Model (4)	Model (5)	Model (6)	Model (7)
Primary in (mm)	L_p=93	93*2	93*3	93*4	93*5	93*6	93*7
	l_p=66	66*2	66*3	66*4	66*5	66*6	66*7
	H_p=23.5	23.5*2	23.5*3	23.5*4	23.5*5	23.5*6	23.5*7
	τ_p=13.2	13.2*2	13.2*3	13.2*4	13.2*5	13.2*6	13.2*7
	l_d=6.9	6.9*2	6.9*3	6.9*4	6.9*5	6.9*6	6.9*7
	H_d=15	15*2	15*3	15*4	15*5	15*6	15*7
	l_e=6.3	6.3*2	6.3*3	6.3*4	6.3*5	6.3*6	6.3*7
Secondary in (mm)	L_s=300	300*2	300*3	300*4	300*5	300*6	300*7
	ls=66	66*2	66*3	66*4	66*5	66*6	66*7
	H_s=1	1*2	1*3	1*4	1*5	1*6	1*7
F[N] .(10^2)	09	16	27	51	75	108	144
P(W)	46	95	133	185	234	277	333

Table-1 Parameters;
L_p: Primary length
l_p: Primary width
H_p: Height of primary
τ_p: No notch
l_d: width of a tooth
H_d: Height of a tooth
l_e: notch width
L_s: Secondary Length
l_s: Secondary width
H_s: Secondary Height